# Reactive Processing of LLDPEs in Corotating Intermeshing Twin-Screw Extruder. II. Effect of Peroxide Treatment on Processability

MARLY G. LACHTERMACHER* and ALFRED RUDIN†

Institute of Polymer Research, Department of Chemistry, University of Waterloo, Waterloo, Ontario, Canada N2L 3G1

SYNOPSIS

Commercial ethylene–octene linear low-density polyethylenes (LLDPEs) were reactively extruded with low levels of a peroxide [2,5-dimethyl-2,5-di(*t*-butylperoxy)hexane] to modify polymer molecular structure and processing properties. Peroxide levels were kept low to avoid crosslinking. This article reports the effects of this reactive extrusion on viscoelastic properties. Rheological properties are more sensitive than are molecular structure characteristics to the changes produced by reactions of very low peroxide concentrations. Complex viscosity increases are seen, especially at low frequencies. Shear-thinning behavior is also accentuated. The crossover between $G'$ and $G''$ moves to lower frequencies. A modified Cole–Cole presentation of these data shows that the elastic component is more predominant for extrusion-reacted materials. Peroxide-modified materials all have higher Bagley end correction values than those of barefoot resins. The former exhibit lower power indices (more shear thinning). All these properties indicate more long-chain branching and higher melt elasticity. However, die swell decreased as a function of peroxide concentration. Peroxide treatment results in an enhancement of elongational viscosity, both under isothermal and cooling conditions, along with a decrease in drawdown ability. The rheological changes parallel those reported earlier in molecular characteristics but are more sensitive and suitable to evaluate the effects of reactive processing. The effectiveness of the reactive extrusion process for improving processability of LLDPEs depends critically on the extrusion conditions. © 1995 John Wiley & Sons, Inc.

## INTRODUCTION

Linear low-density polyethylene (LLDPE) has some processing drawbacks that hamper its extrusion on conventional low-density polyethylene (LDPE) film-blowing equipment. During the extrusion process of LLDPE, the high viscosity at typical extrusion rates is reflected in high levels of screw torque, barrel wear, and melt temperature and in a tendency for melt fracture. Also, LLDPEs exhibit lower extensional viscosity, lower melt strength, and a lower propensity for strain hardening, as reflected in poor bubble stability compared to LDPE with the same melt index.

There is growing interest in the use of low concentrations of organic peroxides as free-radical generators to improve the processability characteristics of polyolefins. Reactive extrusion processes offer a practical route for the peroxide modification of polyolefins. Advantages associated with the reactive extrusion process include considerable processing variability, rapid process changes, and the ability to produce small batches. Tzoganakis et al.[1] reported a comprehensive experimental and theoretical investigation of the free-radical-induced degradation of polypropylene, while Suwanda[2] proposed a mathematical model to predict the changes in molecular weight distribution and gel content of peroxide-modified polyethylene during a single-screw extrusion process.

The present article reports results of a second study in this laboratory on the reactive processing of LLDPEs with peroxides. The first study[3] dem-

* Present address: Petrobras-Cenpes, Ilha do Fundao, Quadra 7, Rio de Janiero, Brasil.

† To whom correspondence should be addressed.

Journal of Applied Polymer Science, Vol. 58, 2433–2449 (1995)
 CCC 0021-8995/95/132433-17

onstrated that reactive extrusion in a corotating intermeshing twin-screw extruder resulted in higher polymer molecular weight, broader molecular weight distribution, and an increase in long-branch concentrations. The changes in carbon–carbon unsaturations are consistent with a reaction scheme in which terminal vinyls dominate the free-radical chain reaction which leads to branching and chain extension. While SEC and $^{13}$C-NMR analyses produce informative data, they are limited in sensitivity compared to thermal measurements (which were reported in the previous article[3]) and to rheological measurements. This article gives details of appropriate rheological characterizations and their application follow changes in molecular structure of LLDPEs during reactive extrusion with low levels of peroxides.

## EXPERIMENTAL

### Materials

The same LLDPEs described in a previous study[3] and designated as Resins A and B were used in this investigation. The organic peroxide, 2,5-dimethyl-2,5-di(*t*-butylperoxy)hexane (Lupersol 101™) used for the chemical reactions of LLDPE resins under investigation was the same as before.[3] As also reported in the previous study, Resin A is similar in molecular structure and rheological properties to Resin B.

In this study, samples are assigned two code numbers: the first corresponding to the resin under investigation, and the second, in brackets, to the peroxide concentration. "Blank" samples in this research were LLDPEs that were extruded without peroxide.

### Extruder Reactor and Methodology

The extruder reactor and the extrusion conditions are the same as detailed in the previous study.[3]

### Rheological Behavior of Virgin Resins and Reactive Extrusion Products

The information gathered for this study involved analyses of the shear flow properties at low shear rates by dynamic mechanical measurements and at higher shear rates on a capillary rheometer. The elongational flow properties of the polymer melts were measured by a non-isothermal melt-spinning technique, described below, and on a Rheometrics uniaxial extensional rheometer.

The viscoelastic properties of virgin samples and reactive extrusion products were measured on a Rheometrics Model 605 mechanical spectrometer. The shear storage modulus $G'(\omega)$ and the shear loss modulus $G''(\omega)$, as well as the complex viscosity $\eta^*(\omega)$, were determined by small-amplitude oscillatory shear experiments in a frequency sweep from $10^{-2}$ to $10^2$ rad/s. Preliminary examinations of reactive extrusion products were performed using a 50 mm cone-and-plate geometry. Dealy and Wissbrun[4] suggested that this geometry is useful mainly for the measurement of the low-shear rate viscosity and the linear viscoelastic properties of melts, which are of interest here.

Sample thicknesses of approximately 1 mm were generated on a hot press at 190°C for 10 min under 20,000 lb force and then used for rheological measurements in a cone-and-plate geometry. Similar results were found for selected reactive extrusion products tested in a parallel-plate geometry, instead of a cone-and-plate setting. The ease of sample preparation and the strong instrumental signal within the range of linear viscoelastic response at a strain level of 10% was the rationale for the use of 50 mm parallel plates in the experiments on further selected resins. Samples evaluated in a parallel-plate geometry were loaded in pellet form and, once melted, were slowly pressed in the rheometer to a thickness of approximately 2 mm. All samples were subjected to an applied strain of 10% at 190°C. The linear viscoelastic region for these resins was evaluated in a strain sweep experiment from 0 to 20% strain at a frequency of 1 rad/s. A plot of the storage modulus $G'(\omega)$ and the loss modulus $G''(\omega)$ as a function of the percentage of strain exhibited a plateau in the linear viscoelastic region of strain. The 10% applied strain used in all experiments was within this region. For each selected resin, three runs were made of oscillatory shear-flow measurements. The average readings of all three replicate runs were used to plot the reported data.

The measured low-frequency limit of complex viscosity $\eta^*(\omega)$ gave the zero-shear rate steady flow viscosity $\eta_0$[5]:

$$\eta^*(\omega \to 0) = \lim \frac{G''(\omega)}{\omega} = \eta_0 \qquad (1)$$

The zero-shear viscosity $\eta_0$ was also determined from the frequency-dependence curve of complex viscosity $\eta^*(\omega)$. This plot exhibited a plateau in the Newtonian region at the lowest frequency, i.e., the measured viscosity is independent of the shear rate. As an operational criterion, this plateau was reached when

the change in the complex viscosity $\eta^*(\omega)$ data with frequency was less than 3%. The zero-shear viscosity $\eta_0$ was determined by extrapolating the plateau values to a zero-frequency limit. Based on this criterion, the flow curves of all selected blank resins exhibited a plateau at the lowest frequency, and the zero-shear viscosity $\eta_0$ of the resins was reported. The absence of a plateau in the flow curves of reactive extrusion products limited the measurement of the zero-shear viscosity $\eta_0$. This observation is an indication of the increased non-Newtonian nature of peroxide-modified LLDPE resins under investigation as compared to the virgin samples. It is known that the zero-shear viscosity $\eta_0$ of resins with broad molecular weight distributions or with a high degree of long-chain branching may be difficult to measure directly using most available commercial rheometers because the shear rate at which $\eta^*(\omega)$ levels out is too low to be generated in these instruments.[4]

The shear flow at high shear rate of selected resins was investigated with a constant rate piston-driven capillary rheometer. The polymer melt was driven by a plunger advancing through the reservoir at a known constant rate, and the force was recorded. The shear stress was calculated from the force values and the length and the area of the plunger. The apparent shear rate was determined by known values of the crosshead speed, the diameter of the plunger, and the diameter of the capillary.[6]

For a non-Newtonian fluid, the apparent shear stress, $\tau_a$, and apparent shear rate $\mathring{\gamma}_a$, are given by the following equations:

$$\tau_a = \frac{\Delta P R}{2L} \tag{2}$$

where $\Delta P$ is the pressure drop, and $R$ and $L$, the radius and the length, respectively, of the capillary, and

$$\mathring{\gamma}_a = \frac{4Q}{\pi R^3} \tag{3}$$

where $Q$ is the volumetric flow rate of the polymer.

Apparent flow curves were determined by plotting log apparent shear stress as a function of log apparent shear rate at a given temperature. The capillary flow analyses of all the selected resins were made at 190°C.

The apparent shear stress $\tau_a$ was corrected to that at the die wall using the method proposed by Bagley.[7] This author suggests that the entrance pressure drop in the capillary could be conveniently handled by imagining it to be equivalent to the effect of an extra length of the capillary tube, expressed as a number of tube diameters. To evaluate the Bagley correction, $e$, for entrance effects, three cylindrical capillary dies, with the same diameter of 1.0 mm and different $L/D$ values ranging from 5 to 20, were used in the capillary flow analysis of resin A before and after peroxide reaction. A plot of the pressure drop $\Delta P$ vs. $L/D$ at a constant apparent shear rate, $\mathring{\gamma}_a$, gave a series of straight lines, one for each constant value of the apparent shear rate. The Bagley entrance correction $e$ was determined by extrapolating such a linear plot to $\Delta P = 0$. The various intercepts at different apparent shear rates $\mathring{\gamma}_a$ gave the correction factor $e$ as a function of $\mathring{\gamma}_a$.

The true shear stress $\tau_w$ at the capillary wall for a given apparent shear rate $\mathring{\gamma}_a$ was calculated by using the following equation:

$$\tau_w = \frac{\Delta P}{2\left(\frac{L}{R} + e\right)} \tag{4}$$

where $e$ is the Bagley entrance correction for the corresponding apparent shear rate.

Correction of the apparent shear rate $\mathring{\gamma}_a$ to that at the capillary wall was accomplished using the method proposed by Rabinowitsch.[8] A logarithmic plot of the true shear stress $\tau_w$ vs. apparent shear rate $\mathring{\gamma}_a$ was generated after applying the Bagley correction for the entrance effect previously described. The slope of this plot yields the Rabinowitsch correction $n$ for the apparent shear rate. The true shear rate at the wall $\mathring{\gamma}_w$ was determined as follows:

$$\mathring{\gamma}_w = \mathring{\gamma}_a\left(\frac{3n + 1}{4n}\right) \tag{5}$$

where $n$ is the Rabinowitsch correction (i.e., $n$ is given as described above). The true flow curves were determined by plotting the log true shear stress at the wall $\tau_w$ as a function of the log true shear rate at the wall $\mathring{\gamma}_w$.

Besides the flow curve analysis, the extrudate swell of selected resins was determined by the capillary extrusion method described by Teh et al.[9] Five samples were cut at each shear rate once the piston force trace exhibited a plateau. The diameter of the 5 cm long air-quenched extrudate was measured approximately 1 cm from the leading end using a micrometer. Two readings of each sample were made. From the 10 measurements, the average extrudate swell was calculated. In addition to shear flow anal-

yses, the elongational flow behavior was investigated by a nonisothermal melt-spinning technique and on an uniaxial extensional rheometer (Rheometrics RER 900).

The nonisothermal melt-spinning experimental procedure used in this work is described by Bailey et al.[10] The polymer was extruded at a constant rate, and the monofilament formed at the die outlet was cooled with refrigerated air, passed through a pulley system, then drawn by a two-roll godet where the filament was wrapped three times. The extruder employed a 1 in. diameter 27 : 1 screw with a 3 : 1 compression ratio. The orifice was a flat entry die with 1.5 mm diameter and $L/D$ of 10. All experiments were carried out at a temperature of 210°C using a constant throughput of approximately 0.1 g/min and three different draw ratios (DR = 5, 8, and 10).

The temperature and the DR range used in the elongational viscosity measurements are appropriate for the processing of polyethylene in film-blowing operations. The draw ratio (DR) was calculated as the ratio of the velocity of the thread at the godet rollers to the average velocity of the melt at the exit of the die. The former velocity was calculated from known values of the surface speed of the godet. In these experiments, the godet speeds were set to 90 and 110 rpm. The velocity of the melt at the die was given by the ratio of the volumetric flow rate $Q$ to the cross-sectional area of the thread at the exit of the die.

The apparent elongational flow resistance $\mu_E$ was calculated based on the flow analysis proposed by Cogswell[11] as follows:

$$\mu_E = \frac{\sigma_z}{\dot{\epsilon}_z} \tag{6}$$

where $\sigma_z$ and $\epsilon_z$ are the tensile stress and the elongational strain rate at a distance $z$ from the die, respectively.

The tensile stress $\sigma_z$ and the elongational strain rate $\dot{\epsilon}_z$ were determined from the following equations:

$$\sigma_z = \frac{F}{\frac{\pi}{4} D_z^2} \tag{7}$$

$$\dot{\epsilon}_z = \frac{Q \ln \left(\frac{r_0}{r_z}\right)^2}{\pi r_z^2 z} \tag{8}$$

where $F$ is the forced applied to the thread; $z$, the distance from the die; $D_z$, the diameter of the thread at a distance $z$ from the die; $Q$, the volumetric flow rate; $r_0$, the initial radius; and $r_z$, the radius at distance $z$ from the die face. The force, $F$, was determined from the measured thread mass using a balance connected to the pulley. The volumetric flow rate $Q$ was calculated as described previously.

This measurement is important because it relates to bubble stability and drawdown in tubular film extrusion.[10] Reactive extrusion with peroxide is employed to improve the former property.

Also, the elongational flow properties were evaluated on a Rheometrics uniaxial extensional rheometer (RER 9000). A cylindrical sample of approximately 6 mm in diameter by 19 mm in length was suspended vertically in a hot silicone oil bath, which was heated uniformly by air blowing through the outer jacket of the glass vessel. The density of the silicone oil was similar to that of the material under investigation to compensate for sample weight and buoyancy, while ensuring uniform temperature distribution. The bottom end of the sample was fixed to a load cell located in the oil bath, and the upper end was attached to a driven rod. The rod was mounted on a high-response linear servodrive with an integral displacement transducer (optical encoder) indicating the sample position and also acting as a feedback element for the servomechanism. Its signal, recorded as a function of time, gave a direct measure of the sample extensional viscosity.

Samples were compression-molded at 190°C for 10 min and then slowly cooled with compressed air at approximately 1°C/min. This procedure was used to maintain the same thermal history among the samples being considered. Cylindrical specimens were generated by machining the annealed samples. Then, the specimens were glued to aluminum mounting clips with a high-temperature Hysol™ brand epoxy adhesive (24 h curing). A specific gravity for the molten resin of 0.773 and 0.761 g/cm$^3$ was used at 170 and 190°C for the sample volume calculations.

The sample deformation was defined in terms of the Hencky strain, as follows:

$$\varepsilon = \ln \left(\frac{L(t)}{L_0}\right) \tag{9}$$

where $L_0$ is the initial sample length, and $L(t)$, the sample length at time $t$. All the experiments were carried out at a given constant strain rate $\dot{\epsilon}$. For this mode, the strain rate $\dot{\epsilon}$ was calculated by the following equation:

$$\dot{\varepsilon} = \frac{d\epsilon}{dt} = \frac{1}{L(t)} \frac{dL(t)}{dt} \tag{10}$$

**Table I Observed Extrusion Process Variables**

| Resin | Torque Reading on Twin Screw Extruder ($N/m^2$) $\times 10^{-5}$ | Lupersol 101* Concentration (% w/w) | Die Pressure ($N/m^2$) $\times 10^{-5}$ |
|---|---|---|---|
| A | 12 | — | — |
| A[0.05] | 16 | 0.05 | — |
| A[0.10] | 17 | 0.10 | — |
| A[0.15] | 18 | 0.15 | — |
| B | 10 | — | 10 |
| B[0.05] | 12 | 0.05 | 16 |
| B[0.10] | 13 | 0.10 | 30 |
| B[0.15] | 14 | 0.15 | 33 |

* 2,5-dimethyl-2,5di(t-butylperoxy)hexane

The tensile stress $\sigma_{11}$ was related to the ratio of the measured force $F$ to the cross-sectional area $A$ of the sample as follows:

$$\sigma_{11}(t) = \frac{FL(t)}{A_0 L_0} \tag{11}$$

The measured elongational stress growth function $\eta_E^+(t)$[12-14] was determined by the following relation:

$$\eta_E^+(t) = \frac{\sigma_{11}(t)}{\dot{\varepsilon}} \tag{12}$$

The uniaxial elongational viscosity $\eta_E$ was defined as the equilibrium value of $\eta_E^+(t)$ in a double logarithmic scale of $\eta_E^+(t)$ as a function of time $t$.

The reactive extrusion products under investigation were also extruded on the same extruder as the one mentioned in the description of the nonisothermal melt-spinning technique, with a slot die (1 in. $L \times 0.39$ in. $W \times 0.042$ in. $H$) at 200°C. Tapes of these samples were generated to investigate the presence of microgel by optical examination.

## RESULTS

It is well known that peroxide-initiated chain extension and branching reactions in polyethylene result in higher melt viscosities. Those effects manifest themselves in an increase of torque levels during the extrusion process.[15] During reactive extrusion, the increases of the torque level and die pressure (Table I) were indeed observed.

Rheological analyses were performed to determine the differences in flow behavior of reactive extrusion products as compared to unreacted ones. Figures 1 and 2 illustrate the plots of complex viscosity as a function of frequency for unreacted extruded resins and reactive extrusion products generated in System 1–Set 1 and System 1–Set 2. A good overlap of replicate runs of Resin A[0.15] and Resin B[0.15] indicated good reproducibility of the complex viscosity measurements. The low-frequency complex viscosity of reactive extrusion products increases as the peroxide concentration is increased (Figs. 1 and 2). The complex viscosity curves shift most when the barefoot polymer is compared with

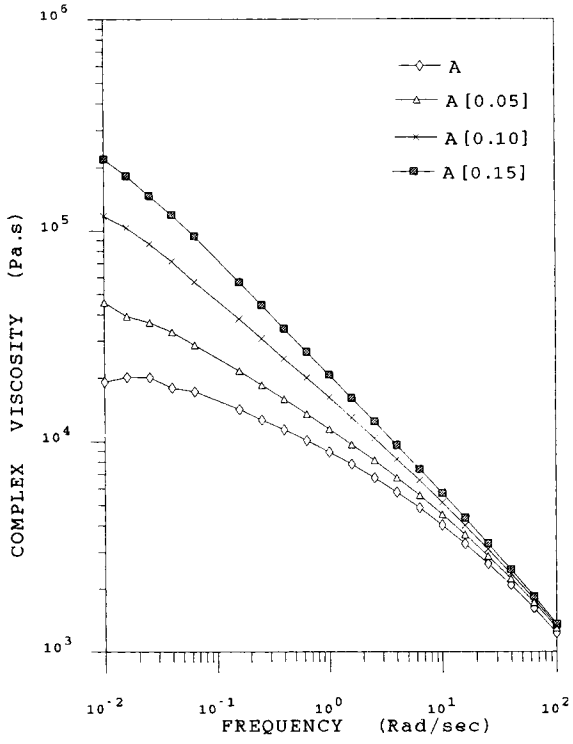


**Figure 1** Complex viscosity as a function of frequency of sample set A[$n$] at 190°C.

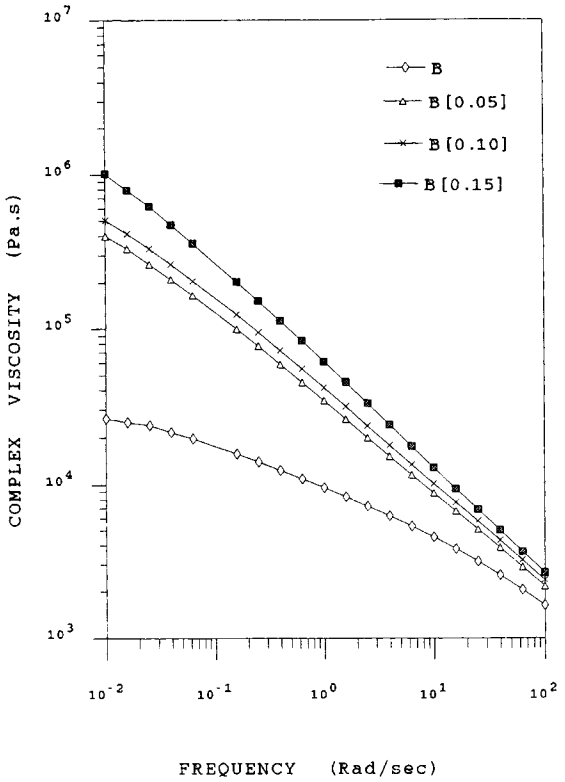


**Figure 2** Complex viscosity as a function of frequency of sample set B[$n$] generated in System 1–Set 2 at 190°C.

that extruded with the lowest peroxide level. Further increases in viscosity are apparent in the products made with successively higher peroxide levels, but the corresponding changes are smaller than the initial shift. These comparisons are in accord with the measured changes in molecular weight distributions, as reported earlier.[3] At higher peroxide concentrations, the SEC measurements of molecular weight distributions did not reveal as pronounced changes as those seen between the blank polymers and the polyethylenes reacted with the lowest peroxide concentration in the experimental range. However, rheological properties are a more sensitive indicator of changes in LLDPE upon peroxide treatment. This is to be expected since the flow properties of a polydisperse material are theoretically[16] proportional to $[(M_{z+1} \cdot M_{z+2})/(M_w \cdot M_z)]$. SEC, on the other hand, is relatively insensitive to higher moments of the molecular weight distributions, which affect $M_{z+}$, and "higher" molecular weight averages.[17]

The enhancement of the low-frequency complex viscosity of peroxide-modified samples, compared to unreacted extruded resins, is consistent with the formation of a low level of long-chain branching in LLDPE resins during the reactive extrusion process. Similar findings are reported by Bersted et al.,[18] although these authors' estimates of log branch concentrations are debatable in view of more modern techniques.

At higher frequencies (above approximately 10 rad/s), the differences between complex viscosities of Resins A[0.05], A[0.10], and A[0.15] compared to Resin A (Fig. 1) are not so significant. A similar trend is revealed for Resins B[0.05], B[0.10], and B[0.15] as compared to Resin B (Fig. 2). Dickie and Koopmans[19] reported that the complex viscosity of an LLDPE at higher shear rates remains unchanged at higher gamma radiation doses, in a parallel observation to ours.

Long branching in polymers is thought to give a more pseudoplastic or shear thinning characteristic to the material as compared to linear analogs. This behavior is shown in plots of complex viscosity as a function of frequency (or shear rate) and for polyethylenes by the greater propensity for LLDPE to reach a Newtonean plateau at low frequencies, compared to LDPE. Such comparisons are made at equivalent melt flow index values according to industrial practice. It should be noted, however, that LDPE will have a broader molecular weight distribution than that of LLDPE with the same melt flow index, and it is difficult to separate the effects of molecular weight distribution and long-chain branching in this case.

Harrell and Nakajima[20] examined the effects of oxidation, shear, and thermally induced reactions in LLDPE during the mixing process (no peroxide was added to the system) on the rheological properties of the resins. These authors concluded that the formation of long-chain branches and the increase of molecular weight produce a low-frequency complex viscosity enhancement. However, in the higher-frequency range, the complex viscosity is not significantly affected. A similar trend is revealed for all reactive extrusion products generated in System 1–Set 1 and in System 1–Set 2, as demonstrated in Figures 1 and 2. Figure 3 demonstrates that the action of peroxide is more drastic for Resins B[0.05] than that of Resin A[0.05]. A similar trend is shown at higher peroxide concentrations for Resin A[0.15] and Resin B[0.15] (Fig. 4). This difference is attributed below to changes in the reactive extrusion process.

Another response of a polymeric melt to stress is elastic flow. Pure elastic response implies that the melt deforms instantly, then reverses instantly. The contribution of the elastic component to the viscoelastic behavior is given by the storage modulus $G'$, while the viscous behavior is represented by the loss

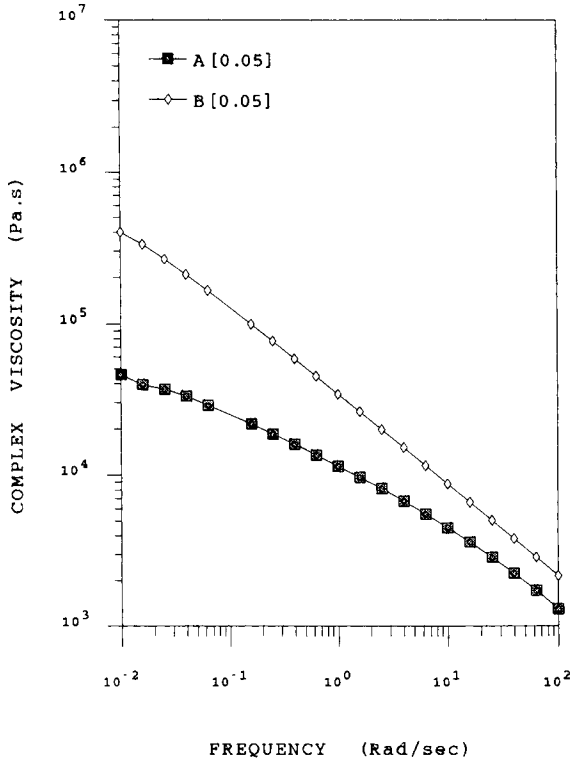


**Figure 3** Complex viscosity as a function of frequency of Resin A[0.05] and Resin B[0.05] at 190°C.

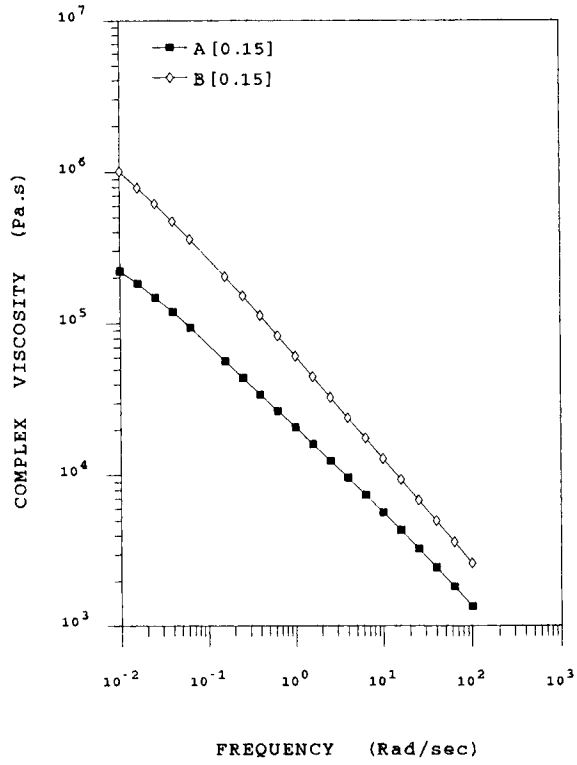


**Figure 4** Complex viscosity as a function of frequency of Resin A[0.15] and Resin B[0.15] at 190°C.

modulus $G''$, as determined by dynamic mechanical spectrometry. Figure 5 illustrates the contribution of both components to the viscoelasticity of Resins A and A[0.05]. The sample codes are assigned to the resin under investigation, and $G'$ and $G''$, to identify the storage component and loss component, respectively. The peroxide concentration follows in brackets. The elastic component $G'$ in Resin A and A[0.05] dominates at the highest frequency, above approximately 100 rad/s. As expected, Resin B (Fig. 6) reveals a similar trend to that of Resin A, since these two resins have similar rheological properties and processability characteristics. The $G'$-$G''$ crossover is shown for Resin B at frequencies above approximately 100 rad/s, while the elastic component $G'$ in Resin B[0.05] becomes more predominant than the viscous response $G''$ at lower frequencies, above approximately 0.04 rad/s (Fig. 6).

The contribution of the elastic response and viscous response to the viscoelastic behavior of reactive extrusion products, generated in both sets, shows a similar trend at higher peroxide concentrations. The $G'$-$G''$ crossover for Resin A[0.10] is shown at a higher frequency, at approximately 16 rad/s more than that for Resin A[0.15], at approximately 0.3

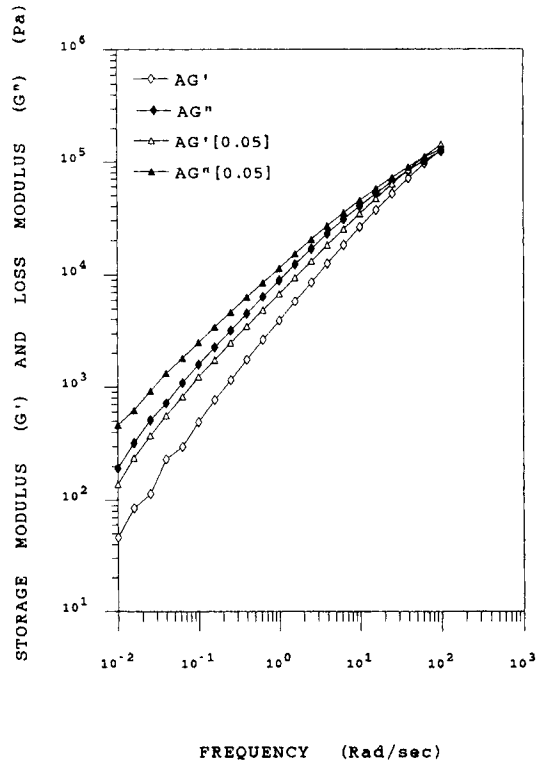


**Figure 5** Storage modulus ($G'$) and loss modulus ($G''$) of Resins A and A[0.05] as a function of frequency at 190°C.

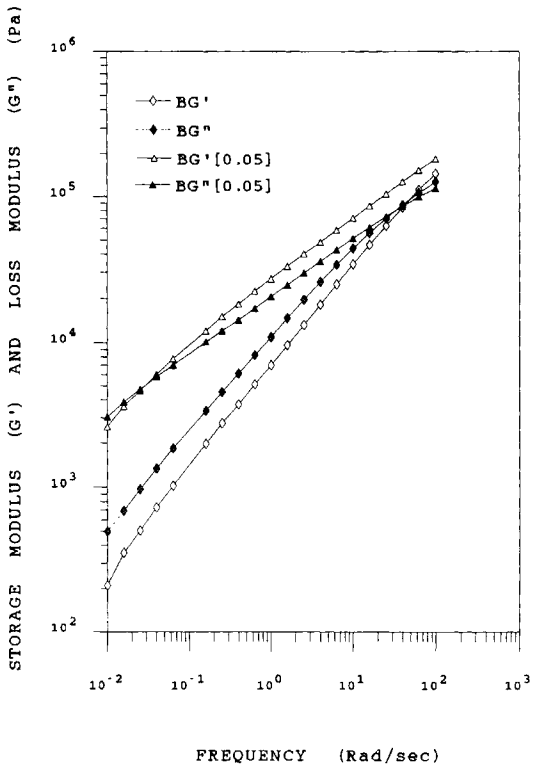


**Figure 6** Storage modulus ($G'$) and loss modulus ($G''$) of Resins B and B[0.05] generated in System 1–Set 2 as a function of frequency at 190°C.

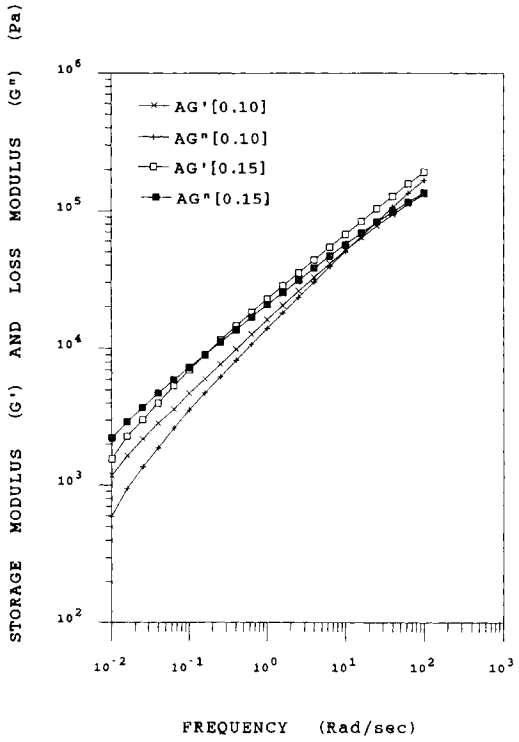


**Figure 7** Storage modulus ($G'$) and loss modulus ($G''$) of Resins A[0.10] and A[0.15] as a function of frequency at 190°C.

rad/s (Fig. 7). A similar trend is exhibited for Resin B[0.10] and Resin B[0.15], as illustrated in Figure 8. The $G'$–$G''$ crossover is shown at approximately 0.03 rad/s for the former resin, while the elastic response $G'$ is dominant over the entire observed frequency range for the latter sample.

Graessley and Roovers[21] reported that in star polystyrenes the crossover of $G'$ and $G''$ occurs at a lower frequency as compared to that in linear polystyrene, suggesting a broader relaxation spectrum for the former polymer. These authors observed that the crossover of $G'$ and $G''$ moves to lower frequency as the molecular weight of the arms increases. This same trend found for the peroxide-modified resins (Figs. 7 and 8) suggests longer relaxation times for the sample after peroxide treatment. This could occur as a result of entanglement of long chains. Wild and co-workers[22] suggested that at low degrees of long-chain branching the viscosity enhancement and the increase of the melt elasticity manifested by the die swell could be explained by the increase of the intermolecular entanglements. Furthermore, Schlund and Utracki[13] suggested that the strain hardening, which is a typical behavior of branched polymers, such as LDPE, could be explained by the presence of a transient network structure produced

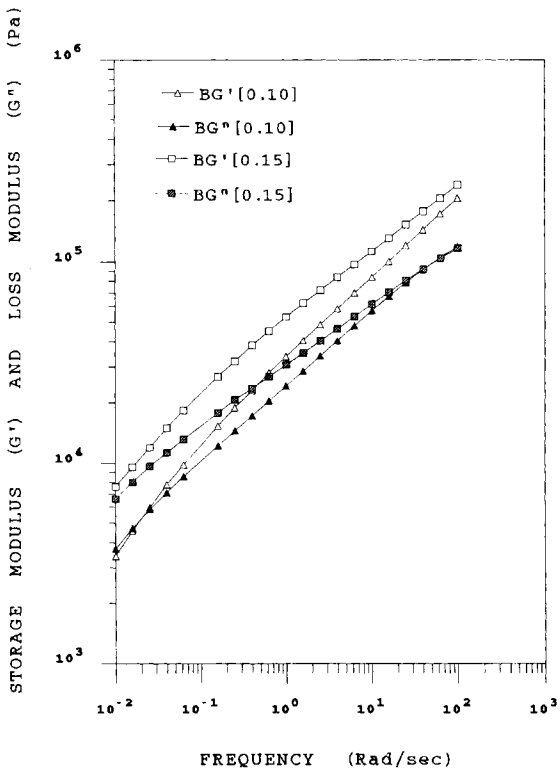


**Figure 8** Storage modulus ($G'$) and loss modulus ($G''$) of Resins B[0.10] and B[0.15] generated in System 1–Set 2 as a function of frequency at 190°C.

by mechanical entanglement of polymeric chains as a result of the presence of long branches. This observation could also explain the increased tendency for strain hardening found in peroxide-modified resins, as will be shown later in this report. Also, the increase of entanglements could explain the increase of the contribution of the elastic characteristic to the viscoelasticity in reactive extrusion products.

The differences in the elastic and the viscous behaviors between the reactive extrusion products generated in System 1–Set 1 and in System 1–Set 2, on the one hand, and the unreacted extruded Resins A and B, on the other hand, demonstrate that low levels of peroxide treatment in LLDPE have a significant effect on the melt-flow behavior of the polymers.

Figure 9 demonstrates that the relative contribution of the elastic component of Resin B[0.05] is more significant than that of Resin A[0.05]. A similar trend is revealed at a higher peroxide concentration for Resins A[0.15] and B[0.15] (Fig. 10). The major difference here is that Resin B was processed in System 1–Set 2, which is more efficient than is Set 1, because of better mixing of components and improved melt temperature control.

Nakajima and Harrell[23] proposed a modified

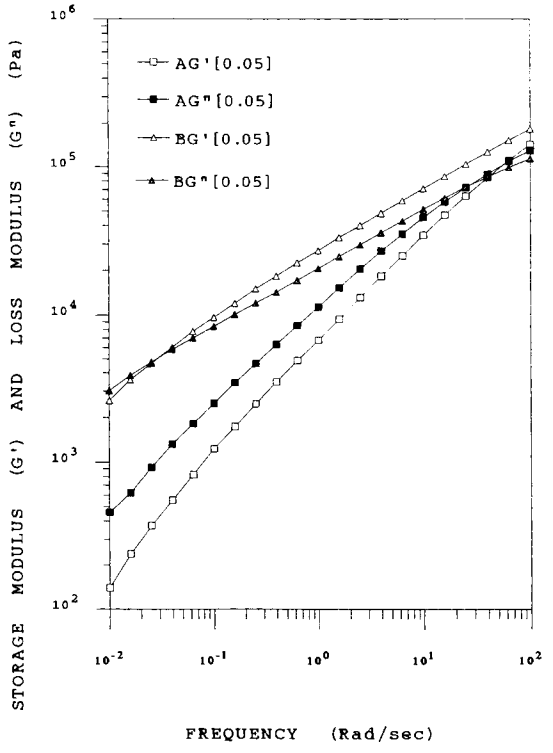


**Figure 9** Storage modulus ($G'$) and loss modulus ($G''$) of Resins A[0.05] and B[0.05] as a function of frequency at 190°C.

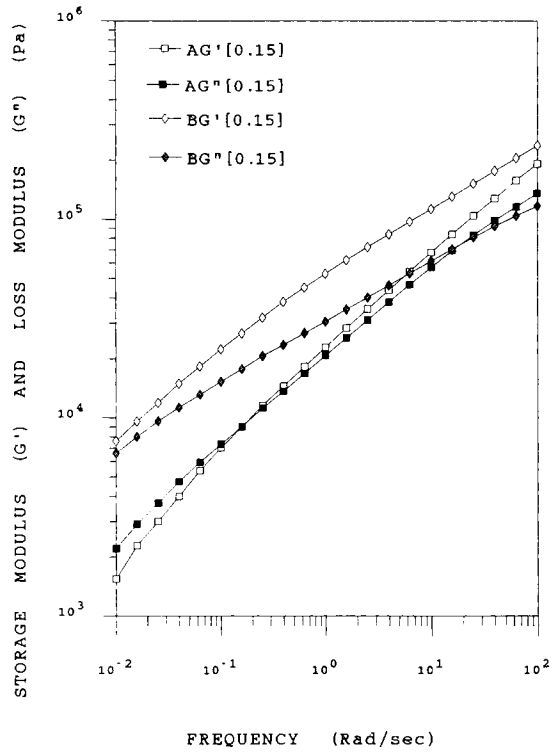


**Figure 10** Storage modulus ($G'$) and loss modulus ($G''$) of Resins A[0.15] and B[0.15] as a function of frequency at 190°C.

Cole–Cole method (mCC), generated by plotting the loss modulus $G''$ as a function of the storage modulus $G'$ in a log–log scale, to represent the relative contribution of the $G'$ response to that of $G''$. On an mCC plot, the data positioned to the right of the equimoduli line $G' = G''$ indicates that the elastic component is the predominant response in the viscoelastic behavior of a polymer. Data located to the left of the equimoduli line shows the opposite effect. Nakajima and Harrell demonstrated that an increase in the degree of long-chain branching is reflected in a shift of the mCC plot toward lower $G''$ values, indicating that the elastic component has a higher relative contribution than that of the viscous response.

According to this interpretation, Figure 11 demonstrates that the degree of long-chain branching in reactive extrusion products generated in System 1–Set 1 increases as the peroxide concentration is increased. Also, these findings show that the elastic response for peroxide-modified resins is more predominant than for the unreacted extruded sample. Figure 12 shows a similar behavior for Resin B before and after peroxide treatment. In comparison to Resins A[0.10] and A[0.15] (Fig. 11), the action of peroxide is more drastic for Resins B[0.10] and B[0.15] (Fig. 12). These results agree with rheo-

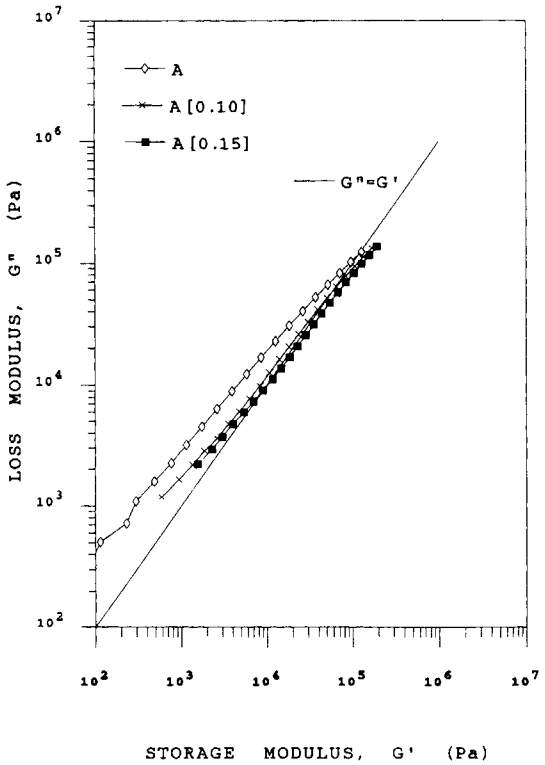


**Figure 11** Loss modulus ($G''$) as a function of storage modulus ($G'$) of Resins A, A[0.10] and A[0.15] at 190°C.

logical measurements reported earlier in this article and with the molecular characterization data given in the preceding article.[3]

The differences in the chemical modification between peroxide-modified resins generated in System 1–Set 1 and in System 1–Set 2 can be attributed to the differences in the extrusion process conditions. It seems that the quality of mixing and the barrel temperature are important variables in peroxide modification of LLDPE through reactive processing. The absence of a water-cooling system in System 1–Set 1, which limited the control of the temperature across the barrel, accounts for the higher melt temperature at the die than that in System 1–Set 2. It is known that higher reaction temperatures favor chain-scission reactions, while lower temperatures favor chain-extension reactions.[24] This is accordance with the results reported in this section, suggesting that the peroxide action was more drastic at the extrusion conditions employed in System 1–Set 2 than those in System 1–Set 1.

In this study, a good incorporation of the peroxide in the polymer melt during the extrusion process is fundamental to generate a homogeneous reactive product. Besides, a homogeneous product is necessary to produce a product with good optical and mechanical properties in film-blowing operations. For this reason, the degree of mixing might affect the kinetic results of reactive extrusion. The effect of the method of dispersion of the peroxide on the chemical modification of LLDPE will be discussed in the next report on reactive process of LLDPEs from this laboratory.

The viscoelastic response of polymer melts at high shear rate is conveniently investigated by capillary flow analysis. The relation between the apparent shear stress and apparent shear rate depends on the die dimensions. The true shear stress at the wall is generated using the Bagley entrance correction. The correction term $e$ is obtained by extrapolating the linear plot of pressure drop vs $L/D$ to $\Delta P = 0$. The Bagley end corrections, $e$, for Resins A before and after peroxide treatment are shown in Table II. The Bagley end corrections tend to increase with the increasing shear rate. A similar trend is reported for LDPEs[9,25] and for high-density polyethylenes (HPPEs).[26] The peroxide-modified samples have higher Bagley end corrections values than those of Resin A at all selected shear rates. These differences are more remarkable as the peroxide concentration is increased, as revealed for Resin A[0.15] (Table II and Figs. 13 and 14). These findings suggest that reactive extrusion products tend to have a higher melt elasticity as compared to those of unreacted

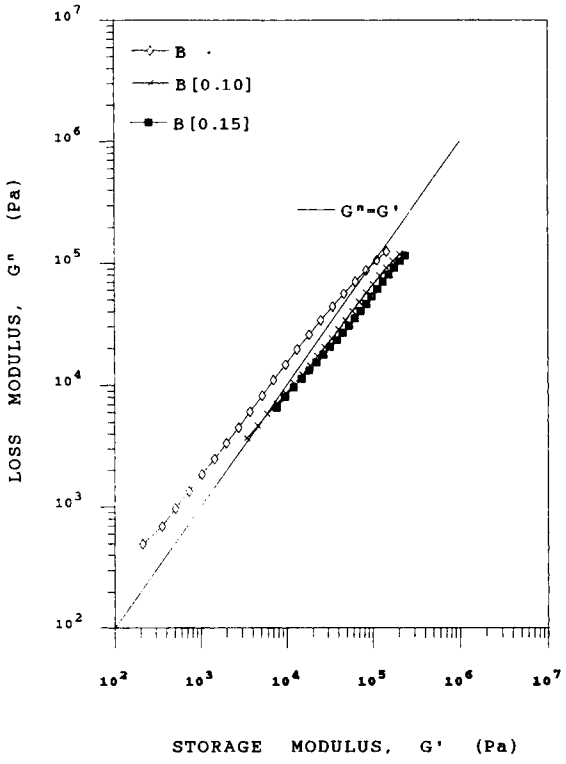


**Figure 12** Loss modulus ($G'$) as a function of storage modulus ($G'$) of Resins B, B[0.10], and B[0.15] at 190°C.

**Table II Bagley End Corrections; Sample Set A[n]**

| Resin | Bagley End Correction | Strain Rate ($s^{-1}$) |
|---|---|---|
| A | 3.33 | 120 |
| A | 4.35 | 240 |
| A | 4.61 | 602 |
| A[0.05] | 3.56 | 120 |
| A[0.05] | 3.42 | 361 |
| A[0.05] | 4.83 | 602 |
| A[0.15] | 4.15 | 120 |
| A[0.15] | 4.36 | 240 |
| A[0.15] | 5.38 | 602 |

extruded resins and correlate with the previous rheological measurements. The latter is demonstrated by the increase of the relative contribution of elastic response in respect to the viscous component for reactive extrusion products generated in System 1–Set 1 as compared to unreacted Resin A (Figs. 5, 7, and 11).

The true shear rate at the wall $\mathring{\gamma}_w$ was generated by applying the Rabinowitsch correction. For the power law fluid, the true shear stress at the wall $\tau_w$ is related to the true shear rate at the wall $\mathring{\gamma}_w$ by the following equation:

$$\tau_w = K\mathring{\gamma}_w^n \tag{13}$$

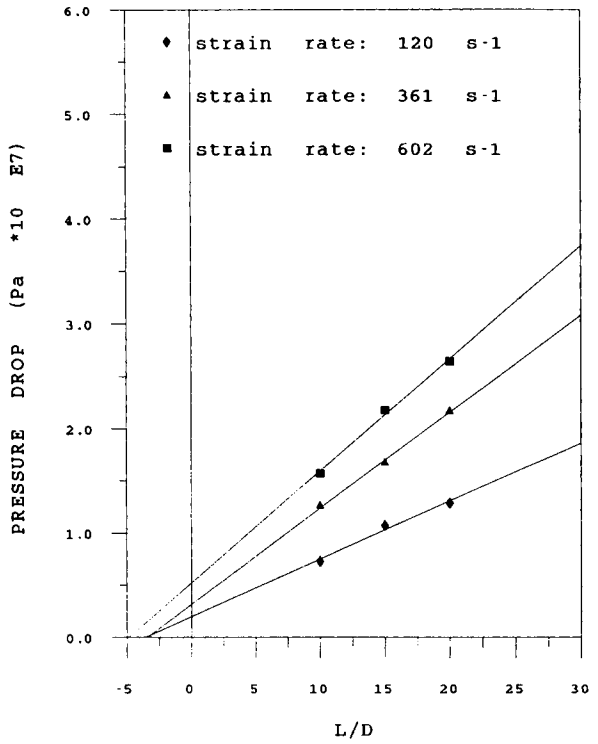


**Figure 13** Bagley plot for determining the end correction for capillary flow of Resin A[0.05].

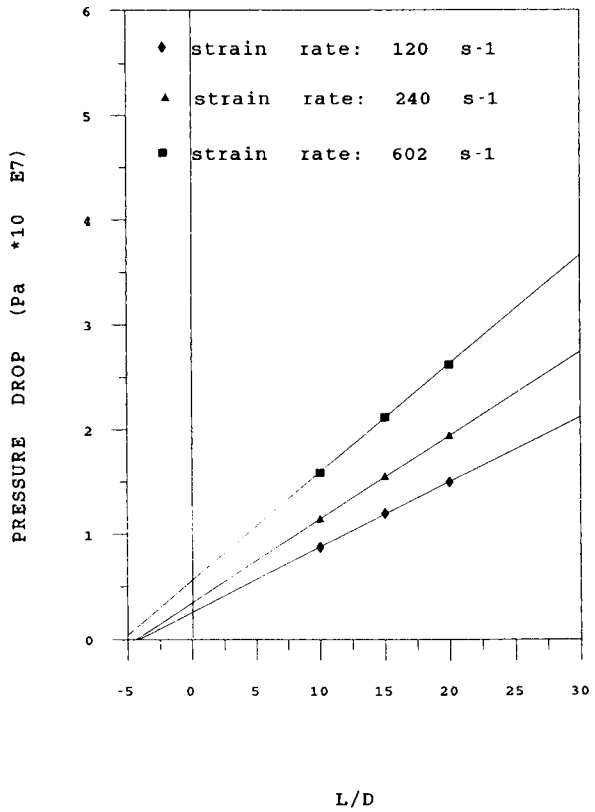


**Figure 14** Bagley plot for determining the end correction for capillary flow of Resin A[0.15].

where $K$ is the consistency parameter, and $n$, the power law index.

On a log $\tau_w$ vs. log $\mathring{\gamma}_w$ plot, a power law fluid is represented by a straight line with slope $n$ and intercept $K$. All selected resins have non-Newtonian characteristics at high shear rate, as indicated by $n < 1$. For a Newtonian fluid, $n$ is 1. It is interesting that Resins A[0.05] and A[0.15] are more pseudoplastic in nature than is Resin A, since the reactive extrusion products exhibit a lower power law index (Table III). Kalyon and Yu[27] suggested that long-chain branching exhibited in LDPE accounts for its lower shear viscosity at high shear rate and its more pseudoplastic nature than those of an LLDPE. These authors mention a lower power law index

**Table III Power Law Parameters of Resins A, A[0.05], and A[0.15]**

| Resin | Consistency Parameter, $K$ (Pa-s $\times 10^{-4}$) | Power Law Index, $n$ |
|---|---|---|
| A | 1.74 | 0.40 |
| A[0.05] | 2.18 | 0.37 |
| A[0.15] | 3.03 | 0.31 |

value for LDPE compared to that of LLDPE. It is apparent that the peroxide treatment of LLDPE resins under investigation is reflected in products that behave more like LDPE.

Figure 15 illustrates the previous complex viscosity measurements as determined by dynamic mechanical spectroscopy (DMS) of Resin A before and after peroxide treatment (Fig. 1), as well as the shear viscosity data generated using capillary flow analysis. In this plot, the sample code is assigned to the resin under investigation and the characterization technique employed is referred to in parentheses. A comparison of the flow curves of Resins A, A[0.05], and A[0.15] determined by these two different methods indicates a similar trend and satisfying coincidence of results.

The flow curves of the unreacted extruded Resin B and the reactive extrusion products generated in System 1–Set 2 are established by using a similar procedure to that of Resin A, before and after peroxide treatment. Resins B and B[0.15], generated in System 1–Set 2, were selected in the evaluation of the effect of peroxide treatment on the capillary flow behavior. The Bagley end correction $e$ was generated using the same procedure detailed previously for all selected resins reacted in System 1–Set 1. Three different capillary dies exhibiting an $L/D$ of 10, 15, and 20 and four shear rates of 120, 240, 361, and 602 $s^{-1}$ were used to perform the Bagley end correction for the entrance effect $e$ for Resin B. To minimize possible uncertainty in extrapolating the pressure drop vs. $L/D$ plots to obtain the correction term, four different capillary dies of $L/D$ 7, 10, 15, and 20 were employed for Resin B[0.15]. It was found that capillary dies of higher $L/D$ deviate from the linear Bagley plot; therefore, they were not used in the calculation of the Bagley end correction. The deviation at long capillary lengths could be due to pressure effects on polymer viscosity or to shear-induced changes in rheological structures in the melt.

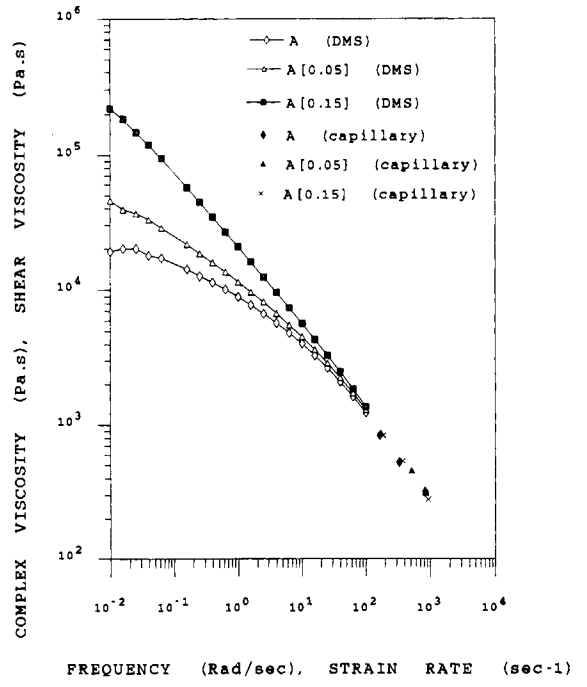


**Figure 15** Viscosity measurements of Resins A, A[0.05], and A[0.15].

Table IV illustrates the Bagley end correction as a function of the shear rate for Resin B and Resin B[0.15]. As for Resin A generated in System 1–Set 1 (Table II), the Bagley end correction tends to increase as the shear rate is increased. The crossover of the Bagley end correction values for Resins B and B[0.15] (Table IV and Fig. 16) can be attributed to the experimental errors associated with these measurements. The Bagley end correction is higher for Resin B[0.15] than for Resin B, at all selected shear rates. A similar trend is revealed for the selected resins generated in System 1–Set 1 (Table II). These results confirm the tendency of peroxide-modified samples to exhibit a higher melt elasticity than that of the unreacted resin.

A similar procedure applied to Resin A was used to perform the Rabinowitsch correction for Resin B before and after peroxide reaction. As expected, the true flow curve of Resin A is similar to that of Resin B, yielding a similar consistency value $K$ and power law index $n$, as expressed in the power law model. The power law index $n$ of Resin B[0.15] is lower than that of the unreacted Resin B (Table IV). The same pattern is shown for Resins A[0.05] and A[0.15] as compared to Resin A (Table III). The action of peroxide in selected LLDPEs results in products with a higher pseudoplastic nature than those of unreacted resins.

In addition to the excess of pressure drop due to entrance capillary flow, the melt elasticity is manifested in the die swell behavior. During the extrusion of polymers through a capillary, the diameter of the extrudate is often found to be larger than the diameter of the capillary, yielding the extrudate swell or die swell phenomenon. This behavior is a manifestation of the elastic response and depends not only on the molecular composition of the melt but also on the melt processability. The die swell of polyethylene resins depends on the die geometry. It decreases as the length to diameter ratio of the capillary increases.

In general, the extrudate swell depends on a combination of molecular weight, MWD, and LCB ef-

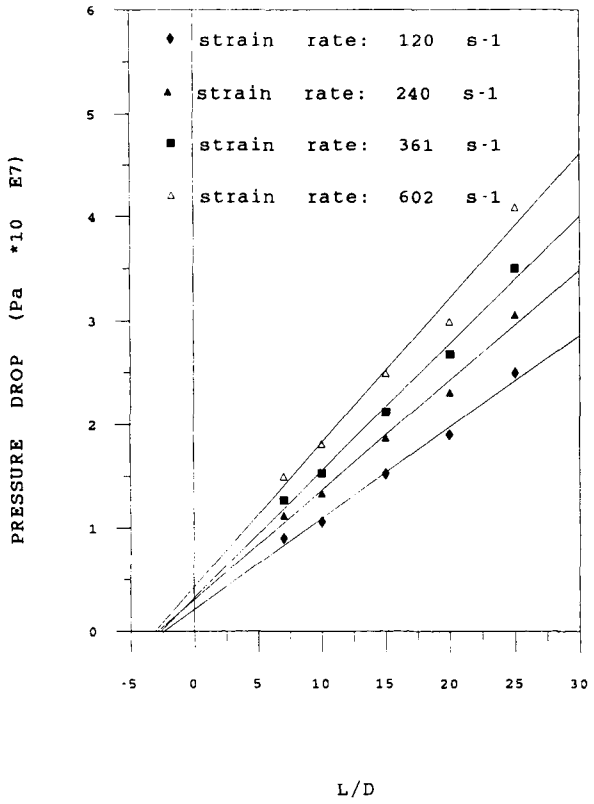


**Figure 16** Bagley plot for determining the end correction in capillary flow of Resin B[0.15].

fects. Contradictory conclusions have been reported about the effects of molecular structure on the extrudate swell behavior of polyethylene. Rogers[28] suggested that the die swell behavior in polyethylene increases with increasing $M_w$ and broadening of the molecular weight distribution. The opposite relationship was reported by Mendelson.[29] Wild et al.[23] and Hamielec and Vlachopoulos[30] suggested that for LDPE with similar molecular weight averages the extrudate swell tends to increase as the degree of long-chain branching increases. In a more recent work, Nakajima and Harrell[23] pointed out that the die swell is not a simple function of the degree of long-chain branching, but that it is affected in a complex manner by branch length and the degree of long-chain branching.

**Table IV Power Law Parameters, Resins B and B[0.15]**

| Resin | Power Law Index, $n$ | Consistency Parameter $K$ (Pa-s $\times$ $10^{-4}$) |
|---|---|---|
| B | 0.41 | 1.76 |
| B[0.15] | 0.27 | 5.28 |

**Table V Power Law Parameters; Resins B and B[0.05]**

| Resin | Bagley End Correction | Strain Rate ($s^{-1}$) |
|---|---|---|
| B | 3.65 | 102 |
| B | 4.39 | 240 |
| B | 4.04 | 361 |
| B | 4.49 | 602 |
| B[0.15] | 3.93 | 120 |
| B[0.15] | 4.78 | 240 |
| B[0.15] | 4.30 | 361 |
| B[0.15] | 5.67 | 602 |

Figure 17 is a plot of the extrudate swell behavior of Resins A before and after peroxide modification in System 1–Set 1 as a function of peroxide concentration at two shear rates and for an $L/D$ capillary die of 10. A similar plot is illustrated in Figure 18, for an $L/D$ capillary die of 20 at three different shear rates. It is interesting that for all conditions studied the die swell tends to decrease with increasing peroxide concentration. If the die swell increases as the degree of long-chain branching is increased, the opposite trend would be expected since peroxide-modified resins have a higher degree of long-chain branching than that of unreacted samples as dem-

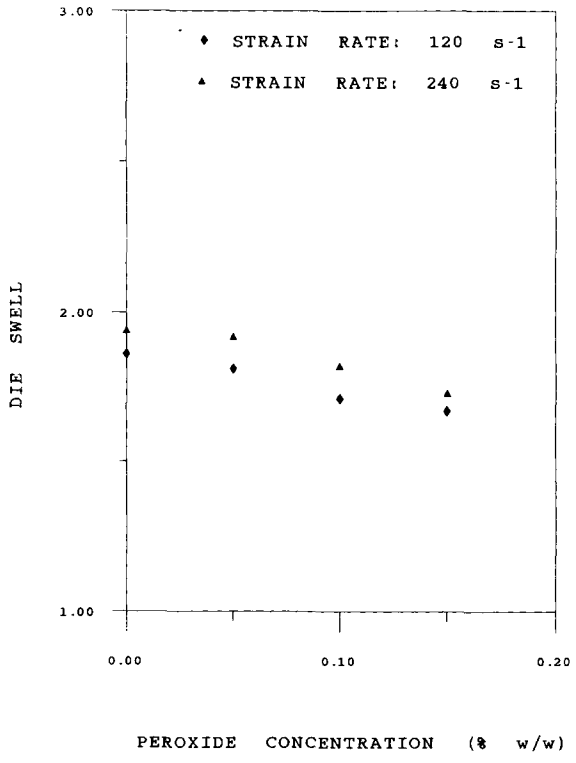


**Figure 17** Die swell as a function of peroxide concentration of sample set A[$n$], cylindrical die, $L/D$ of 10.

onstrated previously. It seems that the melt elasticity of reacted products is affected in a complex manner upon peroxide treatment. It should be noted that no gel was observed for any of the peroxide-modified resins, as determined by an extraction process. Figure 19 demonstrates a similar trend for Resin B before and after peroxide treatment in System 1–Set 2, as measured with an $L/D$ capillary die of 20 and at four strain rates.

The aim of the film-blowing process is to produce a thin film having a uniform gauge and good optical properties. Since the film is quite thin, it is important to avoid the presence in the extrudate of unmelted material (gels) as these will be readily apparent in the finished product. The rheological properties of the polymer melt play an important role in film blowing. They govern the shape and the stability of the bubble and the onset of sharkskin (surface roughness). Drawability, the ability of a melt to be stretched into a thin film without breaking, is associated with extension thinning (strain softening) behavior, while good bubble stability is associated with extension thickening (strain hardening).

Due to the advantage of extreme running simplicity and qualitative information about the effects of some extrusion variables that are important in

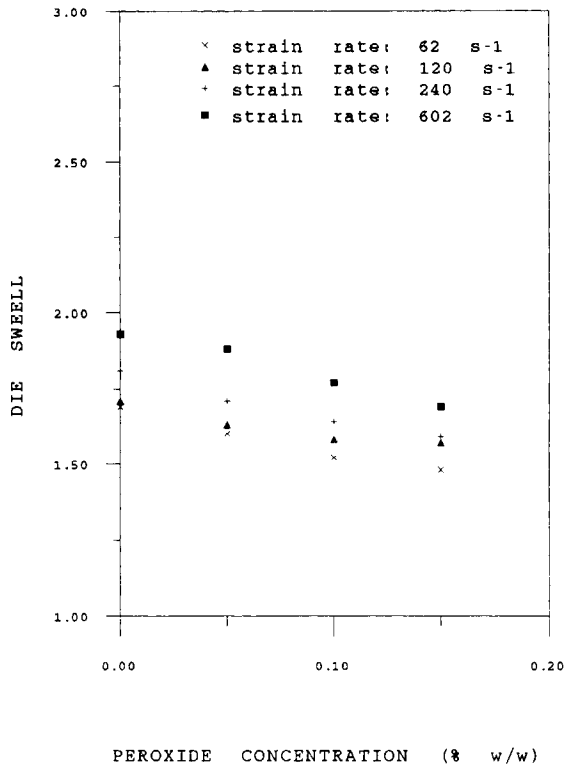


**Figure 19** Die swell as a function of peroxide concentration of sample set B[$n$] generated in System 1–Set 2, cylindrical die, $L/D$ of 20.

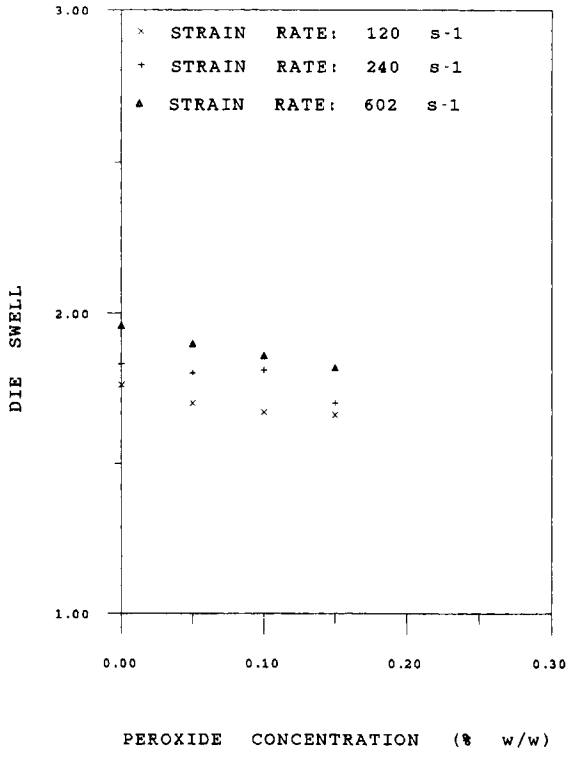


**Figure 18** Die swell as a function of peroxide concentration of sample set A[$n$], cylindrical die, $L/D$ of 20.

film-blowing operations, a non-isothermal melt-spinning technique, described above, was employed to investigate the elongational flow properties of unreacted Resin B and peroxide-modified samples generated in System 1–Set 2.

Generally, three replicate experiments were conducted and filament diameters were averaged as a function of the distance from the die. A linear profile of thread diameters for Resin B as a function of the distance from the die is illustrated in Figure 20, at melt temperature of 210°C, at two draw ratio values. The thread diameter decreases with distance along the spinning way. Resin B[0.10] and Resin B[0.15] exhibited similar profiles.

The maximum value of the draw ratio has been used as a mean of comparing the drawdown characteristics of different material.[31] Resin B is able to be shown to a draw ratio of 22, while the drawdown ability of Resin B[0.10] was limited to a maximum draw ratio of approximately 18. These results can be attributed to the differences in the molecular structure between Resin B and Resin B[0.10]. This effect is more significant at a higher peroxide concentration. While Resin B[0.10] is able to drawdown up to approximately 18 times, the drawdown ability of Resin B[0.15] is limited to a maximum draw ratio

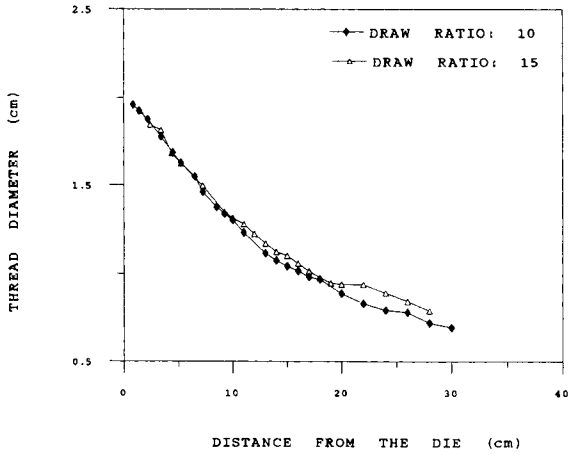


**Figure 20** Filament diameter as a function of die distance for Resin B at draw ratio of 10 and 15 at 210°C.

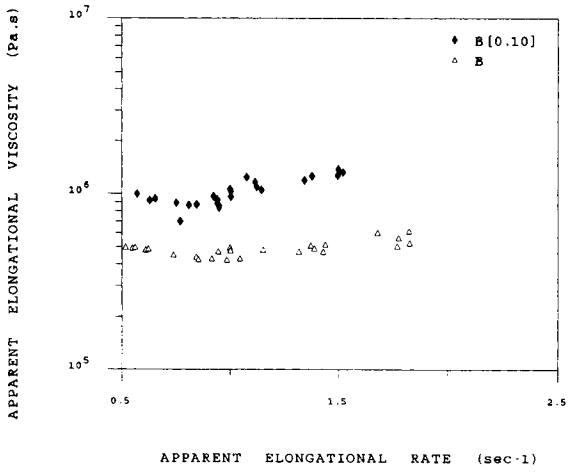


**Figure 21** Apparent elongational viscosity of Resins B and B[0.10] as a function of apparent elongational rate, at draw ratio of 10. Nonisothermal operation.

of approximately 8. These results suggest that the peroxide treatment instigates a decrease in the drawdown ability of peroxide-modified samples, as compared to that of unreacted Resin B.

There are acknowledged drawbacks[32] of the nonisothermal melt-spinning technique in generating information about the rheological properties, since neither the strain nor the temperature are uniform in the filament, and therefore the strain history in the filament is not precisely controlled. However, this objection would apply equally to the film-extrusion process which this experiment simulates. It is interesting to compare the apparent elongational viscosity of peroxide-modified resin to that of unreacted sample. Figure 21 is a plot of the apparent elongational viscosity of Resins B and B[0.10] as a function of the apparent elongational rate, at a draw ratio of 10, when plotted in a semilog scale. The apparent elongational viscosity of Resin B[0.10] is higher than that of Resin B, in the range of observed elongational strain rates. The apparent elongational viscosity of Resin B reaches a plateau at the elongational strain rate above approximately 0.8 $s^{-1}$, while a more steep increase of elongational viscosity for Resin B[0.10], with increasing elongational strain rate, is displayed. The differences in the elongational flow behavior between Resins B and B[0.10] are more pronounced at a higher draw ratio of 15 (Fig. 22). Resin B[0.15] exhibited similar characteristics to B[0.10].

In addition, the isothermal uniaxial extensional flow behavior of Resin B before and after peroxide treatment was evaluated on the Rheometrics extensional rheometer at a Hencky strain of 3.1. The extensional viscosity of Resin B[0.15] is displayed in a double logarithmic scale as a function of time at four strain rates at 190°C (Fig. 23). Figure 24 illustrates the stress growth function of Resins B and B[0.15] at $\dot{\epsilon}$ of 0.03 $s^{-1}$ at 190°C. Resin B[0.15] exhibits a significant higher extensional viscosity as compared to Resin B. This result is in agreement with previously elongational flow analysis as determined by a nonisothermal melt-spinning technique. In addition, the extensional viscosity of Resin B tends to level off at high strain, while a steeper increase of the extensional viscosity of Resin B[0.15] indicates a higher tendency of this resin for strain hardening as compared to Resin B (Fig. 24). However, the increase of the extensional viscosity of peroxide-modified resin seems to be at the expense of its drawdown ability. This observation is shown by a lower deformation range for Resin B[0.15] as com-

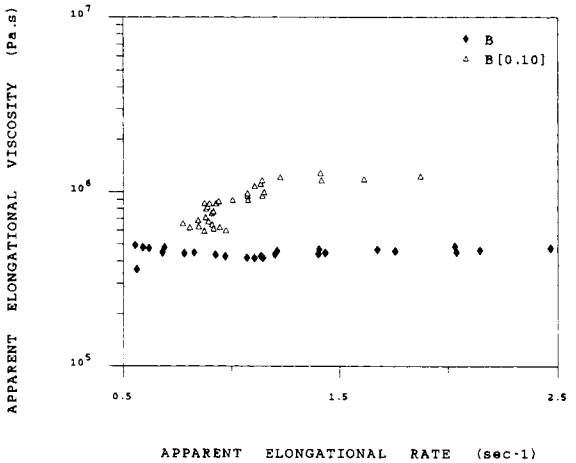


**Figure 22** Apparent elongational viscosity of Resins B and B[0.10] as a function of apparent elongational rate, at draw ratio of 15. Nonisothermal operation.

pared to that for Resin B. At $\dot{\epsilon}$ of 0.03 $s^{-1}$, the former resin breaks at a strain of approximately 0.8, while the latter one breaks at a strain of approximately 3.0. These results agree with the previous flow analysis measured by the nonisothermal melt-spinning technique.

The elongational flow measurements indicate the action of peroxide in selected LLDPEs results in products with higher elongational viscosity but a lower drawdown ability. It is evident that peroxide treatment in the LLDPE under investigation plays an important role not only in the shear flow properties of modified peroxide samples but also in their extensional flow behavior.

## CONCLUSIONS

The first study of this research[3] demonstrated that molecular weight averages tend to increase with increasing peroxide concentration. Also, the reacted samples tend to exhibit a broader molecular weight distribution, which seems to be related to a higher degree of long-chain branching. These results are corroborated in the present investigation by an increase of the shear thinning nature of polymer melts as shown by the enhancement of the low-frequency complex viscosity and by a decrease of the power law index values, as well as by an increase of the contribution of the elastic response to the viscoelasticity for the extrusion products. Also, the increase of the Bagley end correction values for the resins after peroxide treatment suggest an increase of the melt elasticity. In addition, the use of a modified Cole–Cole plot to assess variations in molecular structure, such as molecular weight distribution, and

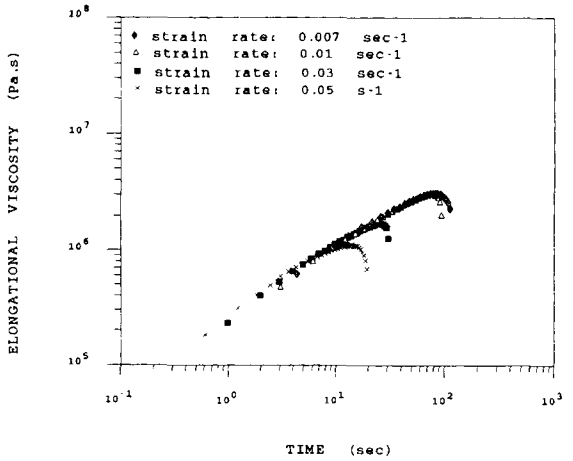


**Figure 23** Extensional viscosity as a function of time of Resin B[0.15], at 190°C.

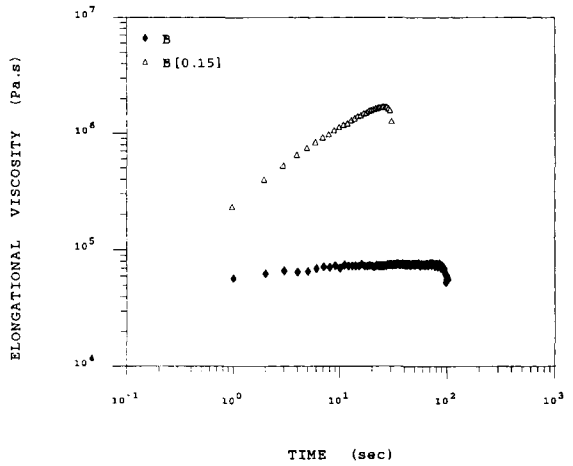


**Figure 24** Extensional viscosity as a function of time of Resins B and B[0.15], at $\dot{\epsilon}$ of 0.03 $s^{-1}$, at 190°C.

the degree of long-chain branching, suggested that long-chain branching was induced in LLDPE when treated with reactive extrusion peroxide.

The changes in the molecular characteristics of LLDPEs upon peroxide treatment affected not only their shear flow properties but also their elongational flow behavior. For example, Resins B[0.10] and B[0.15] generated in System 1–Set 2 have a higher elongational viscosity as well as a higher tendency for strain hardening than those of unreacted Resins B. However, at the highest peroxide concentration, the improvements in the elongational flow properties are limited by a decrease in the drawdown ability. For example, Resin B[0.15] exhibits a higher elongational viscosity than that of Resin B[0.10], but the drawability is lower for the former resin.

The effectiveness of the reactive extrusion process for improving the processability of LLDPE seems to be dependent upon the extrusion conditions, such as the temperature and the quality of mixing. For example, the extrusion conditions used in System 1 were satisfactory in achieving a homogeneous product. However, a better control of the temperature and a better mixing during reactive processing employed in System 1–Set 2 as compared to those in System 1–Set 1 can explain the more drastic action of the peroxide treatment for the products generated in the former system.

Based on the results obtained in this work, the measurements of the rheological properties are revealed to be more sensitive to evaluate the effects of reactive processing of LLDPEs as compared to measurements of polymer molecular structure.[3]

This research was supported by the Natural Science and Engineering Research Council of Canada. M.G.L. is grateful to CNPQ and Petrobras for scholarship support.

## REFERENCES


1. C. Tzoganakis, J. Vlachopoulus, and A. E. Hamielec, *Polym. Plast. Technol. Eng.*, **28**(3), 319 (1989).
2. D. Suwanda, PhD Thesis, Department of Chemical Engineering, University of Toronto, 1992.
3. M. G. Lachtermacher and A. Rudin, to appear.
4. J. M. Dealy and K. F. Wissbrun, *Melt Rheology and Its Role in Plastics Processing*, Van Nostrand Reinhold, New York, 1990, pp. 277–279.
5. S. Rosen, *Fundamental Principles of Polymeric Materials*, Wiley, New York, 1981, pp. 263–264.
6. E. C. Bernhardt, *Processing of Thermoplastic Materials*, Van Nostrand Reinhold, New York, 1959.
7. E. B. Bagley, *J. App. Phys.*, **28**(5), 624 (1957).
8. B. Rabinowitsch, *Z. Phys. Chem.* A, **145,** 1 (1929).
9. J. W. Teh, A. Rudin, and H. P. Schreiber, *Plast. Rubb. Process. Appl.*, **4**(2), 149 (1984).
10. L. Bailey, D. Cook, J. O. Pronovost, and A. Rudin, *Polym. Eng. Sci.*, **34,** 1485 (1993).
11. F. N. Cogswell, *Rheol. Acta*, **8,** 187 (1969).
12. B. Schlund and L. A. Utracki, *Polym. Eng. Sci.*, **27,** 380 (1987).
13. B. Schlund and L. A. Utracki, *Polym. Eng.*, **27**(20), 1523 (1987).
14. D. M. Kalyon and D. S. Czerwonka, *Plast. Rubb. Process. Appl.*, **14,** 29 (1990).
15. S. Ultsch and H. G. Fritz, *Plast. Rubb. Proc. Appl.*, **13,** 81 (1990).
16. R. B. Bird, C. F. Curtiss, R. C. Armstrong, and O. Hassager, *Dynamics of Polymer Liquids*, 2nd ed., Wiley, New York, 1987.
17. S. Balke, *Quantitative Column Chromatography*, Elsevier, Amsterdam, 1984.
18. B. H. Bersted, J. D. Slee, and C. A. Richter, *J. Appl. Polym. Sci.*, **26,** 1001 (1981).
19. B. D. Dickie and J. Koopmans, *J. Polym. Sci. Part C*, **28,** 193 (1990).
20. E. R. Harrell and N. Nakajima, *J. Appl. Polym. Sci.*, **29,** 995 (1984).
21. W. W. Graessley and J. Roovers, *Macromolecules*, **12,** 959 (1979).
22. L. Wild, R. Ranganath, and D. C. Knobeloch, *Polym. Eng. Sci.*, **16,** 811 (1976).
23. N. Nakajima and E. R. Harrell, in *Current Topics in Polymer Science*, R. M. Ottenbrite, L. A. Utracki, and S. Inoue, Eds., Hanser, Munich, 1987, Vol. 2, p. 149.
24. T. Bremner and A. Rudin, *Plast. Rubb. Process. Appl.*, **13,** 61 (1990).
25. A. P. Metzer and R. S. Rodkey, *J. Appl. Polym. Sci.*, **7,** 399 (1963).
26. R. C. Pentwell, R. S. Porter, and S. Middleman, *J. Polym. Sci. A-2*, **9,** 731 (1971).
27. D. M. Kalyon and D. W. Yu, *Polym. Eng. Sci.*, **28,** 1542 (1988).
28. M. G. Rogers, *J. Appl. Polym. Sci.*, **14,** 1679 (1970).
29. R. A. Mendelson, *J. Appl. Polym. Sci.*, **19,** 1061 (1975).
30. L. A. Hamielec and J. Vlachopoulos, *J. Appl. Polym. Sci.*, **28,** 2389 (1983).
31. C. D. Han, *Rheology in Polymer Processing*, Academic Press, San Diego, CA, 1976.
32. K. F. Wissbrun, *Polym. Eng. Sci.*, **13,** 342 (1973).


*Received February 21, 1995*
*Accepted June 6, 1995*